

***In Silico* Evaluation of Antidiabetic Activity and ADMET Prediction of Compounds from *Musa acuminata* Colla Peel**

Xenia Erika N. Bucao* and Judilynn N. Solidum

Department of Pharmaceutical Chemistry, University of the Philippines Manila
Manila, Metro Manila 1000 Philippines

Diabetes is a severe chronic disease that affects 422 million adults worldwide in 2014. It was the fifth leading cause of mortality in the Philippines in 2019. The primary cause of death of diabetic patients is due to cardiovascular disease. α -Glucosidase inhibitors (AGIs) are known for their cardiovascular benefits because they prevent the postprandial glucose level from increasing, which plays a significant role in the development of cardiovascular diseases. The synthesis of AGIs is complex and requires a lot of steps. Thus, there is a need to explore and discover AGIs especially from plants, which are known sources of bioactive compounds. Drug discovery entails a complex, costly, time-consuming, and risky process. Computer-aided drug discovery/design (CADD) methods such as molecular docking and ADMET (absorption, distribution, metabolism, excretion, and toxicity) prediction have been developed to identify the promising compounds that will be tested in *in vitro* and *in vivo* experiments. This shortens the research process and helps reduce the expense and risk of failure for drug discovery. In this study, molecular docking was conducted to predict the α -glucosidase inhibitory activity of compounds from *Musa acuminata* Colla peel against human intestinal α -glucosidase. Out of 87 compounds, only 11 compounds were found to have better or comparable binding affinity with the standard, acarbose (-8.8 kcal/mol) – namely, sesamin (-9.8 kcal/mol), asarinin (-9.7 kcal/mol), quercetin-7-rutinoside (-9.4 kcal/mol), kaempferol-3-rutinoside (-9.4 kcal/mol), (-)-epicatechin (-9.0 kcal/mol), (+)-catechin (-8.9 kcal/mol), myricetin-3-rutinoside (-8.9 kcal/mol), quercetin (-8.9 kcal/mol), kaempferol-3-rhamnoside-7-glucoside (-8.9 kcal/mol), stigmasterol (-8.9 kcal/mol), and β -sitosterol (-8.8 Kcal/mol). The prediction of ADMET properties and drug-likeness revealed how the best binding compounds may behave inside the body. Some of the compounds were found to be safe and have good absorption, distribution, metabolism, and excretion properties. They showed promising potentials that may lead to their development as drugs.

Keywords: α -glucosidase, ADMET prediction, diabetes, molecular docking, *Musa acuminata* Colla peel

INTRODUCTION

Diabetes is a serious chronic disease that affects 422 million adults worldwide in 2014 (WHO 2016b). Over time, diabetes can lead to several complications in the heart, blood vessels, eyes, kidneys, and nerves when

not managed properly (ADA 2011; WHO 2018). It is an important public health problem for it is one of four priority non-communicable diseases that are responsible for almost 70% of all deaths worldwide (WHO 2016b). In fact, diabetes was also the fifth leading cause of mortality in the Philippines in 2019 (PSA 2021).

The primary cause of death of diabetic patients is due to cardiovascular disease (WHO 2016a). AGIs are

*Corresponding Author: xnbcuao@gmail.com
xnbcuao@up.edu.ph

competitive inhibitors of alpha-glucosidase enzymes, which hydrolyze carbohydrates into glucose, consequently delaying glucose absorption in the gastrointestinal tract. The delayed carbohydrate absorption allows extended time for β -cells to increase insulin secretion (Bharathkumar *et al.* 2014). This prevents the postprandial glucose level from increasing, which plays a significant role in the development of cardiovascular diseases (Joshi *et al.* 2015; Jiang *et al.* 2017). Thus, there is an urgent need to discover AGI from plants since they are known sources of bioactive compounds (Etsassala *et al.* 2020) and they are more accessible to people, especially to those who are in remote areas who use plants as their primary treatment (Singab *et al.* 2014).

Musaceae (banana family) is one of the most important fruit crops cultivated in tropical countries because of its role in the food industry (Padam *et al.* 2014). In the tropical island of Mauritius, *M. acuminata* Colla is used as a remedy against diabetes and related complications by native people by eating the ripe fruit half in the morning and the other half in the evening daily (Mootoosamy and Mahomoodally 2017). The variety of phytochemicals present in *M. acuminata* Colla plant parts may be accountable for their therapeutic effects and justify their use as traditional medicine against various diseases and ailments (Mathew and Negi 2016). The ethanolic extract of its inner peels was found to exhibit significant antihyperglycemic activity in Wistar rats compared to other *Musa* species (Navghare and Dhawale 2016). In addition, the major triterpenes – cycloeucalenone and 31-norcycloclaudenone – present in its peels was reported to possess inhibitory activity against yeast α -glucosidase (Shang *et al.* 2021). Most of the bananas are cultivated primarily for their fruit. As a result, large quantities of underutilized by-products such as peels are generated, which can cause serious ecological damages if not properly managed (Padam *et al.* 2014; Vu *et al.* 2017). Exploring valuable uses of banana peel, like using it as a source of active compounds that may be developed into a drug, may help lessen these wastes.

Drug discovery entails a complex, costly, time-consuming, and risky process (Leelananda and Lindert 2016). CADD methods such as molecular docking and ADMET prediction have played an important role in drug discovery over the past decades. These methods have been developed to speed up the research process and help reduce the expense and risk of failure for drug discovery (Ou-Yang *et al.* 2012).

Molecular docking enables researchers to efficiently investigate the behavior of ligands in the binding site of the target protein, receptor, or enzyme with a considerable degree of accuracy (Hajalsiddig *et al.* 2020). The main goal of this analysis is to determine the best possible pose

of the ligand with minimal binding energy (Anthony *et al.* 2016). The interaction between the ligand and the enzyme may predict the enzyme inhibition or activation activity since it is assumed that the biological activity of the ligand is associated with the binding affinity of the ligand to the enzyme (Xiang *et al.* 2012; Dar and Mir 2017).

Around 40% of the total drug failures in clinical phases are attributed to poor ADMET properties (Durán-Iturbide *et al.* 2020). The *in silico* prediction of ADMET properties in the early phase of drug discovery extremely reduces these failures (Daina *et al.* 2017). This also helps save time and resources, since the experimental evaluation of these properties is time-consuming and expensive (Macalino *et al.* 2015).

The study was conducted to assess the α -glucosidase inhibitory potential of compounds from *M. acuminata* Colla peel. Molecular docking was performed to determine the *in silico* α -glucosidase inhibitory activity of the compounds against human intestinal α -glucosidase. ADMET properties and drug-likeness prediction of the best binding compounds, which have better or comparable binding affinity to the standard acarbose was also carried out. To the best of the researchers' knowledge, there are no foreign and local studies conducted yet concerning the molecular docking and pharmacokinetic prediction of compounds found in *M. acuminata* Colla peel. Thus, this study can serve as a guide and source of information for the scientific community about the compounds' potential as AGIs.

MATERIALS AND METHODS

Data Collection

The dataset used in this study was composed of 87 compounds from *M. acuminata* Colla peel identified in published literature (Someya *et al.* 2002; Mokbel and Hashinaga 2005; González-Montelongo *et al.* 2010; Villaverde *et al.* 2013; Rebello *et al.* 2014; Niamah 2015; Mordi *et al.* 2016; Barroso *et al.* 2019; Navghare *et al.* 2019). The 3D structure data file (sdf) of some compounds was downloaded from the PubChem database (<https://pubchem.ncbi.nlm.nih.gov/>). Compounds that do not have an available sdf in PubChem were manually drawn using Biovia Discovery Studio Visualizer version 21.1.0.20298 or DS Visualizer.

Enzyme Preparation

The crystal structure of human intestinal α -glucosidase in complex with acarbose PDB (protein data bank) ID: 3TOP was retrieved in pdb file format from the RCSB PDB (<https://www.rcsb.org/>). Water molecules and heteroatoms, including the co-crystallized acarbose, were

removed from the α -glucosidase using the DS Visualizer because these can affect the docking accuracy (Opo *et al.* 2021). Since the α -glucosidase (3TOP) is a symmetrical dimer, chain B of the enzyme was removed, and only chain A was used in the docking process (Figure 1). The pre-processed enzyme was then prepared at UCSF Chimera (Pettersen *et al.* 2004) where hydrogens were added. The incomplete side chains were also replaced using Dunbrack 2010 rotamer library (Shapovalov and Dunbrack 2011) and typed with Gasteiger charges. AMBER ff14sb was added to the standard residues of the enzyme (Chukwuemeka *et al.* 2021). The enzyme file was saved in pdbqt format. The prepared human intestinal α -glucosidase is simply referred to as α -glucosidase throughout the rest of the paper.

Ligand Preparation

Each of the 87 ligands, in sdf file, were prepared using the DS Visualizer. Hydrogens were added to the ligands, then the ligands were typed with Merck molecular force field (MMFF) and saved as pdb files. The ligand files were converted to pdbqt file using Open Babel tool (O'Boyle *et al.* 2011) in PyRx.

Molecular Docking

The binding site residues were determined using DS Visualizer with reference to the co-crystallized acarbose and according to Ren and co-authors (2011), the depositor of the 3TOP α -glucosidase–acarbose complex in PDB. The molecular docking was done using AutoDock Vina in PyRx version 0.8 (Trott and Olson 2010; Dallakyan and Olson 2015). AutoDock Vina is simply referred to as Vina throughout the rest of the paper.

The standard acarbose was extracted from the α -glucosidase. Hydrogens and MMFF charges were added to it using DS Visualizer. The prepared acarbose was repeatedly re-docked to the binding site of the α -glucosidase by using different grid box and exhaustiveness parameters to determine the best method that produces a pose with low root mean square deviation (RMSD) when compared to the co-crystallized acarbose. A pose with RMSD lower than 1.5Å was considered a good pose (Rentzsch and Renard 2015). The 87 ligands were docked to the α -glucosidase following the validated docking method done to acarbose. The ligands were docked one at a time to gather their individual binding affinities (kcal/mol).

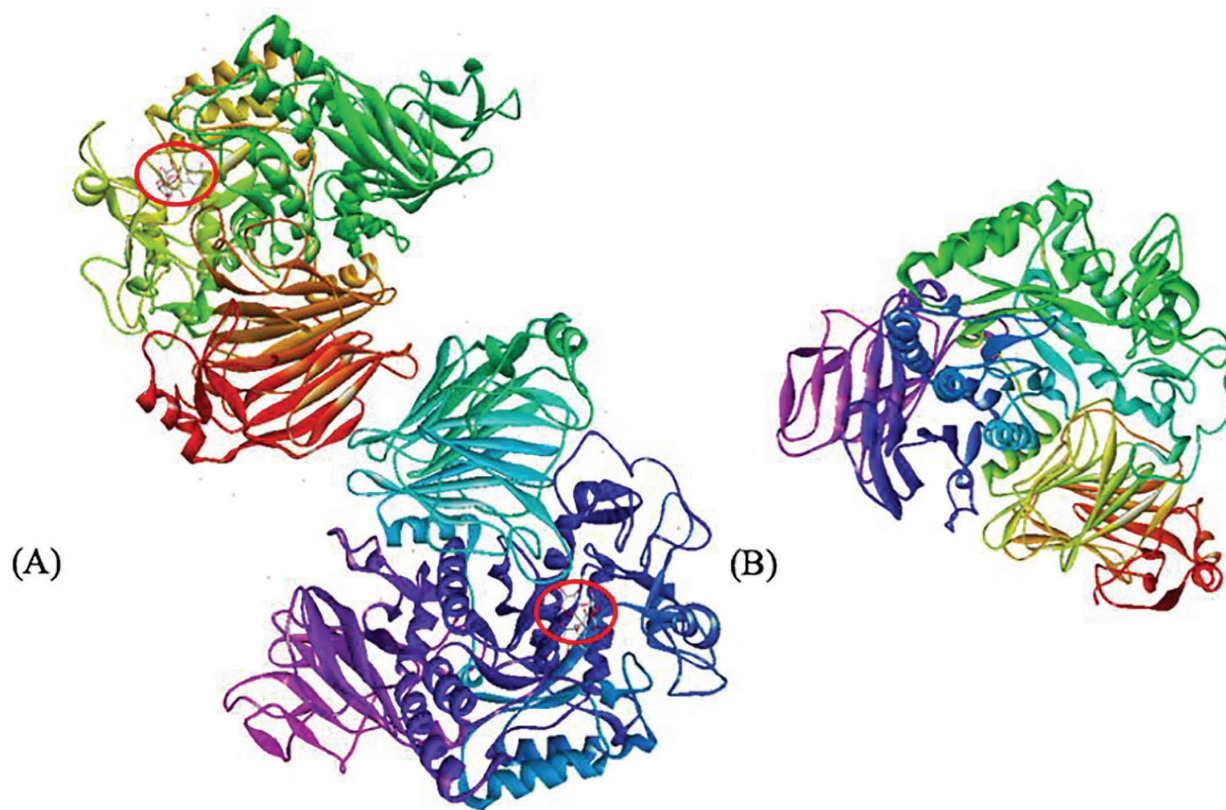


Figure 1. (A) Structure of 3TOP: human intestinal α -glucosidase in complex with acarbose (encircled) and (B) prepared α -glucosidase that was used in molecular docking.

ADMET and Drug-likeness Prediction

The simplified molecular input line entry system (SMILES) of each compound was copied from PubChem and was loaded to SwissADME (Daina *et al.* 2017) and pkCSM (Pires *et al.* 2015) cheminformatics web tools to calculate their ADMET properties. Drug-likeness and Lipinski parameters were also predicted by SwissADME.

RESULTS AND DISCUSSION

Molecular Docking

The molecular docking method was validated by re-docking the extracted acarbose to the α -glucosidase before docking the 87 ligands. This was to ensure that the method gives reliable docking results for the 87 ligands when docked to the binding site of the α -glucosidase. The determination of binding site amino acid residues is important in setting the grid box parameters. The determined binding site residues were ASP1157, TYR1251, ASP1279, TRP1355, TRP1369, TRP1418, ASP1420, MET1421, ARG1510, ASP1526, PHE1559, PHE1560, and HIS1584. The grid parameter was set to center grid box values of X = -33.441, Y = 31.865, and Z = 29.320 and dimensions (Å) of X = 16.064, Y = 18.762, and Z = 17.537. The exhaustiveness, which controls the

comprehensiveness of the Vina search, was set to 16. After the docking run, Vina returned nine different poses. The lower the numerical values for the binding affinity, the better is the predicted binding between the ligand and the enzyme (Dallakyan and Olson 2015). Thus, the pose of re-docked acarbose which had the lowest binding affinity of -8.8 kcal/mol was chosen as the best pose. The heavy atom RMSD of the re-docked acarbose to the co-crystallized acarbose that was computed using DockRMSD web tool (Bell and Zhang 2019) was 0.842Å. This showed that the re-docked Acarbose and later, the ligands, were bound to the binding site of α -glucosidase where the co-crystallized acarbose was bound and that the docking method conducted was appropriate (Rentzsch and Renard 2015). Figure 2 shows the overlay of the re-docked acarbose and co-crystallized acarbose poses in the α -glucosidase binding site.

The re-docked Acarbose (-8.8 kcal/mol) was bound to α -glucosidase residues by five hydrogen bonds and two hydrophobic interactions (Table 1). Hydrogen bonds are very important in ligand-enzyme interactions because they stabilize the ligand in the binding pocket (Kostal 2016; Abelian *et al.* 2021). They also contribute to the specificity of the ligand-enzyme interactions (Safitri *et al.* 2020). The binding site residues common in providing hydrogen bonds to both re-docked and co-crystallized acarbose are ASP1157, ASP1279, ARG1510, and ASP1526. One unfavorable

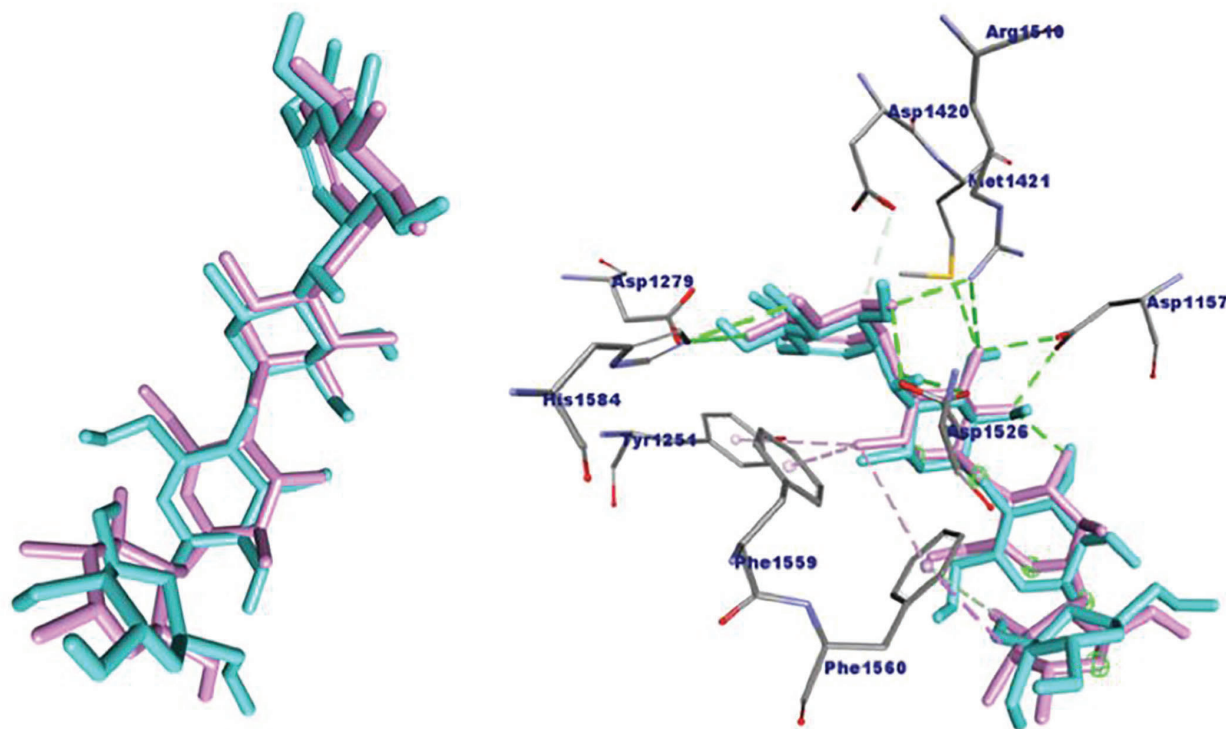


Figure 2. The re-docked (light blue line) and the co-crystallized (pink line) poses of acarbose in the α -glucosidase binding site.

Table 1. Interaction of the best binding compounds with α -glucosidase binding site residues.

Best binding compounds	Binding affinity (kcal/mol)	No. of H-bonds	Interaction	Category
Sesamin	-9.8	3	A:LYS1460:HZ1 - N:Lig:O (2.99 Å)	Hydrogen bond
			N:Lig:C - A:ASP1526:OD2 (3.78 Å)	Hydrogen bond
			N:Lig:C - A:ASP1157:OD1 (3.39 Å)	Hydrogen bond
			A:TYR1251 - N:Lig (5.07 Å)	Hydrophobic
			A:TRP1369 - N:Lig (5.28 Å)	Hydrophobic
			A:TRP1369 - N:Lig (5.21 Å)	Hydrophobic
			A:PHE1559 - N:Lig (4.89 Å)	Hydrophobic
Asarinin	-9.7	3	A:LYS1460:HZ1 - N:Lig:O (2.57 Å)	Hydrogen bond
			A:LYS1460:HZ3 - N:Lig:O (2.25 Å)	Hydrogen bond
			N:Lig:C - A:ASP1420:OD2 (3.29 Å)	Hydrogen bond
			A:TRP1355 - N:Lig (5.96 Å)	Hydrophobic
			A:TRP1355 - N:Lig (5.31 Å)	Hydrophobic
			A:TYR1251 - N:Lig (4.95 Å)	Hydrophobic
			N:Lig - A:PRO1159 (4.69 Å)	Hydrophobic
Quercetin-7-rutinoside	-9.4	3	A:TYR1251:HH - N:Lig:O (2.01 Å)	Hydrogen bond
			N:Lig:H - A:ASP1526:OD1 (2.55 Å)	Hydrogen bond
			N:Lig:H - A:ASP1279:OD2 (2.67 Å)	Hydrogen bond
			A:ASP1526:OD2 - N:Lig (4.40 Å)	Electrostatic
			A:MET1421:SD - N:Lig (5.87 Å)	Other (pi-sulfur)
			A:TRP1369 - N:Lig (5.86 Å)	Hydrophobic
			A:TYR1251 - N:Lig (5.05 Å)	Hydrophobic
			A:TRP1355 - N:Lig (5.09 Å)	Hydrophobic
			A:PHE1560 - N:Lig (5.09 Å)	Hydrophobic
			A:ARG1510:HH11 - N:Lig:H (1.96 Å)	Unfavorable
			A:HIS1584:HE2 - N:Lig:H (1.32 Å)	Unfavorable
Kaempferol-3-rutinoside	-9.4	5	A:GLN1372:HE22 - N:Lig:O (2.21 Å)	Hydrogen bond
			A:ARG1377:HH22 - N:Lig:O (2.69 Å)	Hydrogen bond
			A:LYS1460:HZ3 - N:Lig:O (1.99 Å)	Hydrogen bond
			N:Lig:H - A:ASP1157:O (1.96 Å)	Hydrogen bond
			N:Lig:H - A:GLY1365:O (2.28 Å)	Hydrogen bond
			A:TYR1251 - N:Lig (5.16 Å)	Hydrophobic
			A:PHE1559 - N:Lig (4.78 Å)	Hydrophobic
			A:PHE1560 - N:Lig (4.84 Å)	Hydrophobic
			N:Lig - A:PRO1159 (4.95 Å)	Hydrophobic
(-)-Epicatechin	-9.0	2	A:THR1586:HG1 - N:Lig:O13 (1.98 Å)	Hydrogen bond
			N:Lig:H4 - A:ASP1157:OD1 (1.98 Å)	Hydrogen bond
			A:PHE1427 - N:Lig (5.57 Å)	Hydrophobic
			A:TYR1251 - N:Lig (4.98 Å)	Hydrophobic
			A:PHE1559 - N:Lig (5.00 Å)	Hydrophobic
			A:ASP1279:OD1 - N:Lig:O21 (2.98 Å)	Unfavorable
(+) -Catechin	-8.9	3	N:Lig:H - A:ASP1279:OD2 (2.15 Å)	Hydrogen bond
			N:Lig:H - A:ASP1157:OD1 (2.55 Å)	Hydrogen bond
			A:PRO1159:CD - N:Lig:O (3.66 Å)	Hydrogen bond
			A:PHE1560 - N:Lig (5.32 Å)	Hydrophobic
			N:Lig - A:PRO1159 (5.38 Å)	Hydrophobic

Best binding compounds	Binding affinity (kcal/mol)	No. of H-bonds	Interaction	Category
Myricetin-3-rutinoside	-8.9	5	A:TYR1251:HH - N:Lig:O (2.69 Å)	Hydrogen bond
			A:ARG1510:HH12 - N:Lig:O (2.91 Å)	Hydrogen bond
			A:ILE1587:HN - N:Lig:O (2.77 Å)	Hydrogen bond
			N:Lig:H - A:ASP1157:O (2.07 Å)	Hydrogen bond
			A:PRO1159:CD - N:Lig:O (3.42 Å)	Hydrogen bond
			A:TYR1251 - N:Lig (5.52 Å)	Hydrophobic
			A:PHE1560 - N:Lig (4.91 Å)	Hydrophobic
			N:Lig - A:PRO1159 (4.89 Å)	Hydrophobic
Quercetin	-8.9	2	N:Lig:H - A:ASP1279:OD2 (2.41 Å)	Hydrogen bond
			N:Lig:H - A:ASP1157:OD1 (2.60 Å)	Hydrogen bond
			A:ASP1526:OD2 - N:Lig (4.96 Å)	Electrostatic
			A:TYR1251 - N:Lig (4.93 Å)	Hydrophobic
			A:TRP1355 - N:Lig (5.00 Å)	Hydrophobic
			A:PHE1560 - N:Lig (5.57 Å)	Hydrophobic
Kaempferol-3-rhamnoside-7-glucoside	-8.9	4	A:ARG1510:HH11 - N:Lig:O (2.27 Å)	Hydrogen bond
			N:Lig:H - A:ASP1157:OD2 (2.77 Å)	Hydrogen bond
			N:Lig:H - A:ASP1526:OD2 (2.44 Å)	Hydrogen bond
			N:Lig:H - A:ASP1420:OD2 (2.26 Å)	Hydrogen bond
			A:ASP1526:OD1 - N:Lig (4.78 Å)	Electrostatic
			A:ASP1526:OD1 - N:Lig (4.60 Å)	Electrostatic
			A:TYR1251 - N:Lig (5.43 Å)	Hydrophobic
			A:TRP1355 - N:Lig (4.89 Å)	Hydrophobic
			A:PHE1559 - N:Lig (5.09 Å)	Hydrophobic
			A:PHE1559 - N:Lig (4.91 Å)	Hydrophobic
			A:HIS1584:HE2 - N:Lig:H (1.13 Å)	Unfavorable
Stigmasterol	-8.9	0	N:Lig:C - A:TYR1251 (3.46 Å)	Hydrophobic
			A:TYR1251 - N:Lig (5.12 Å)	Hydrophobic
			A:TRP1355 - N:Lig (5.11 Å)	Hydrophobic
			A:PHE1559 - N:Lig (5.45 Å)	Hydrophobic
			A:PHE1560 - N:Lig (4.86 Å)	Hydrophobic
β-Sitosterol	-8.8	0	A:TYR1251 - N:Lig (4.69 Å)	Hydrophobic
			A:TRP1355 - N:Lig (5.38 Å)	Hydrophobic
			A:TRP1355 - N:Lig (5.28 Å)	Hydrophobic
			A:TRP1369 - N:Lig (4.47 Å)	Hydrophobic
			A:TRP1369 - N:Lig (4.95 Å)	Hydrophobic
			A:PHE1559 - N:Lig (5.00 Å)	Hydrophobic
Acarbose	-8.8	5	A:ARG1510:HH11 - N:Lig:O (2.24 Å)	Hydrogen bond
			N:Lig:H - A:ASP1157:OD1 (2.14 Å)	Hydrogen bond
			N:Lig:H - A:ASP1526:OD2 (2.09 Å)	Hydrogen bond
			N:Lig:H - A:ASP1279:OD2 (2.09 Å)	Hydrogen bond
			N:Lig:H - A:ASP1279:OD1 (2.05 Å)	Hydrogen bond
			N:Lig:C - A:PHE1560 (3.69 Å)	Hydrophobic
			A:PRO1159 - N:Lig (5.19 Å)	Hydrophobic
			A:THR1528:HG1 - N:Lig:H (1.66 Å)	Unfavorable

interaction was also present, as shown in Figure 3A. This unfavorable interaction may be due to the PyRx software treating the α -glucosidase as a rigid structure and the ligand as flexible, so there might be an induced-fit effect causing the clashes between the residues and the docked ligand (Ramachandran *et al.* 2011). Unfavorable interactions might affect the activity and stability of the complex binding (Dhorajiwala *et al.* 2019), but one or two unfavorable interactions are negligible (Zainab *et al.* 2020a, b).

The 87 ligands were docked one at a time to the α -glucosidase using the validated docking method. The poses returned by Vina with the lowest binding energy for each of the ligands were picked as their best poses. Out of 87 ligands, only 11 were found to have a better and same binding affinity with the standard, Acarbose (Table 1).

Among the 11 top compounds, sesamin has the lowest and best binding affinity, which is -9.8 kcal/mol. It was found that sesamin was stabilized by three hydrogen bonds with LYS1460, ASP1526, and ASP1157 plus four hydrophobic interactions with TYR1251, TRP1369, and PHE1559 residues. On the other hand, asarinin or episesamin – the epimer of sesamin – was found to have a binding affinity of -9.7 kcal/mol and was stabilized by three hydrogen bonds with LYS1460 and ASP1420, and four hydrophobic interactions with TRP 1355, TYR1251, and PRO1159. Both sesamin and acarbose formed hydrogen bonds with ASP1157 and ASP1526.

Quercetin-7-rutinoside belongs to the flavonoid-7-o-glycosides class, while kaempferol-3-rutinoside belongs to flavonoid-3-o-glycosides (TMIC 2019b, d). Quercetin-7-rutinoside and kaempferol-3-rutinoside both have a binding affinity of -9.4 kcal/mol. Quercetin-7-rutinoside

was stabilized by three hydrogen bonds with TYR1251, ASP1526, and ASP 1279; four hydrophobic interactions with TRP1369, TYR1251, TRP1355, and PHE1560; one electrostatic interaction with ASP1526; and one pi-sulfur interaction with MET1421. Its interactions with ARG1510 and HIS1584 were found to be unfavorable. The amino acid residues that are common in providing hydrogen bond and hydrophobic interactions to both quercetin-7-rutinoside and acarbose are ASP1526, ASP1279, and PHE1560. The interaction of kaempferol-3-rutinoside with α -glucosidase, on the other hand, was stabilized by five hydrogen bonds and four hydrophobic interactions. The amino acid residues that provided these interactions are GLN1372, ARG1377, LYS1460, ASP1157, GLY1365, TYR1251, PHE1559, PHE1560, and PRO1159. Both kaempferol-3-rutinoside and acarbose formed hydrogen bonds and hydrophobic interactions with ASP1157, PHE1560, and PRO1159. Kaempferol-3-rutinoside was found to be more potent than the standard Acarbose in inhibiting α -glucosidase from *S. cerevisiae* (Habtemariam 2011).

(-)-Epicatechin is a monomeric flavan-3-ols, which is a subclass of flavonoids (Neilson and Ferruzzi 2011). Its consumption was found to reduce blood glucose levels in diabetic patients, but its exact mechanism of action is still being explored (Abdulkhaleq *et al.* 2017). The docking of (-)-epicatechin to α -glucosidase resulted in a binding affinity of -9.0 kcal/mol. It was stabilized by two hydrogen bonds with THR 1586 and ASP1157, and three hydrophobic interactions with PHE1427, TYR1251, and PHE1159. It was also found that its interaction with ASP1279 resulted in an unfavorable interaction. The amino acid residue common in providing hydrogen bond to both (-)-epicatechin and acarbose is ASP1157.

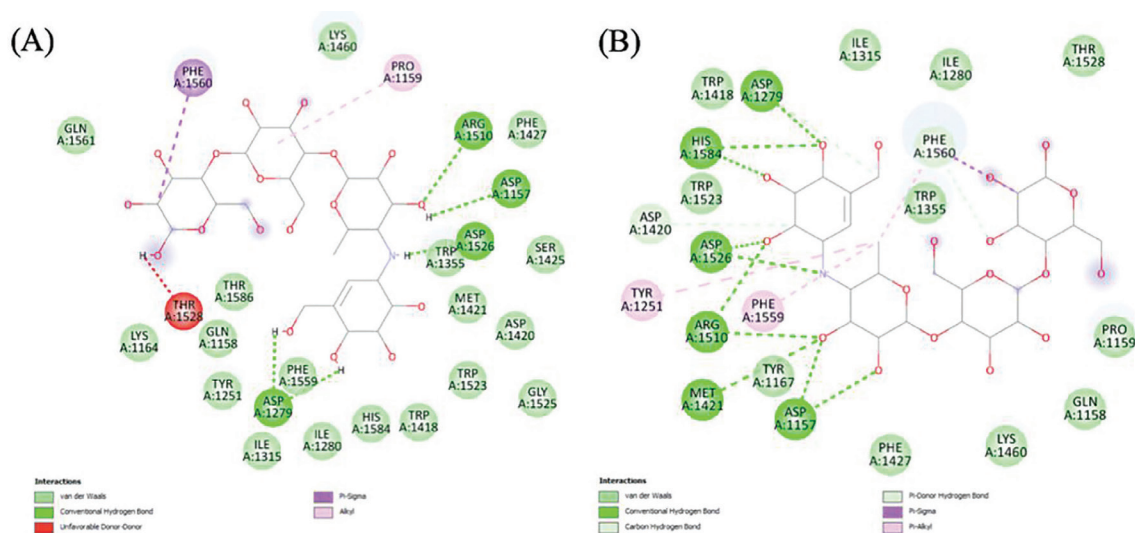


Figure 3. Interactions between the (A) re-docked and the (B) co-crystallized acarbose with the binding site residues of α -glucosidase as visualized in DS Visualizer.

(+)-Catechin is also a monomeric flavan-3-ols like its isomer, epicatechin (Neilson and Ferruzzi 2011). Its antidiabetic effect by enhancing the antioxidant defense system of the diabetic rat models was reported in the study of Samarghandian and co-authors (2017). It has a binding affinity of -8.9 kcal/mol – same with those of myricetin-3-rutinoside, quercetin, kaempferol 3-rhamnoside-7-glucoside, and stigmasterol. Its binding to α -glucosidase was stabilized by three hydrogen bonds with ASP1279, ASP1157, and PRO1159 plus two hydrophobic interactions with PHE1560 and PRO1159. Both (+)-catechin and acarbose interacted with ASP1157, ASP1279, PHE1560, and PRO1159 *via* hydrogen bonding and hydrophobic interactions.

Myricetin-3-rutinoside, a member of the class flavonoid-3-o-glycosides (TMIC 2019c). Its interaction with α -glucosidase was stabilized by five hydrogen bonds with TYR1251, ARG1510, ILE1587, ASP1157, and PRO1159 plus three hydrophobic interactions with TYR1251, PHE1560, and PRO1159. Myricetin-3-rutinoside and acarbose have similar hydrogen bond and hydrophobic interactions with ASP1157, PHE1560, and PRO1159.

The interaction of quercetin – a flavonol – to α -glucosidase was stabilized by two hydrogen bonds plus three hydrophobic and one electrostatic interaction. The interacting amino acid residues were ASP1279, ASP1157, TYR1251, TRP1355, PHE1560, and ASP1526. In addition, the amino acid residues common in providing hydrogen bonds and hydrophobic interaction to both quercetin and Acarbose are ASP1279, ASP1157, ASP1256, and PHE1560. It was reported to have an inhibitory effect against intestinal α -glucosidases in *in vivo* rat models and *in vitro* intestinal homogenates of rats in the study of Pereira and co-authors (2011).

Kaempferol-3-rhamnoside-7-glucoside belongs to the flavonoid-7-o-glycosides class (TMIC 2019a). It was stabilized by four hydrogen bonds with ARG1510, ASP1157, ASP1526, and ASP1420; two electrostatic interactions with ASP 1526; and four hydrophobic interactions with TYR1251, TRP1355, and PHE1559. An unfavorable interaction of kaempferol 3-rhamnoside-7-glucoside with HIS1584 was also found. Both kaempferol-3-rhamnoside-7-glucoside and acarbose interacted with ARG1510, ASP1157, and ASP1526 – forming hydrogen bonds.

Stigmasterol and β -sitosterol are phytosterols that were found to have an antidiabetic activity by restoring β -cells of diabetic rat models, thus stimulating the secretion of insulin (Ramu *et al.* 2016). Stigmasterol and β -sitosterol were also reported to have good inhibitory activity against α -glucosidase from *S. cerevisiae* with an IC50 (half-maximal inhibitory concentration) of 158.25 μ M or 65.31 ± 0.37 μ g/mL (Murugesu *et al.* 2018) and against

α -glucosidase from *Bacillus stearothermophilus* with an IC50 of 1258.35 mg/L (Sheng *et al.* 2014), respectively. In this study, stigmasterol was found to have five hydrophobic interactions with TYR1251, TRP1355, PHE1559, and PHE1560 residues. Both stigmasterol and acarbose formed hydrophobic interactions with PHE1560. On the other hand, β -sitosterol has six hydrophobic interactions with TYR1251, TRP1355, TRP1369, and PHE1559 residues of α -glucosidase. β -Sitosterol interaction with α -glucosidase leads to a binding affinity of -8.8 kcal/mol, which is similar to acarbose, as shown in Table 1.

ADMET and Drug-likeness Prediction

The ADMET properties and drug-likeness of the best binding compounds predicted by pkCSM and SwissADME cheminformatics tools are presented in Table 2.

Absorption. Water solubility is an important property that influences absorption (Ottaviani *et al.* 2010; Daina *et al.* 2017). All of the best binding compounds were predicted to be water-soluble except for stigmasterol and β -sitosterol, which are poorly soluble.

The Caco2 or human epithelial colorectal adenocarcinoma cell lines are widely used as *in vitro* models to predict the absorption of an orally administered drug in the human intestinal mucosa. Compounds with high Caco2 permeability have greater than 0.90 predicted values (Pires *et al.* 2015). Only sesamin, asarinin, kaempferol-3-rutinoside, stigmasterol, and β -sitosterol were predicted to have high Caco2 permeability.

The intestine is considered to be the primary site for absorption of an orally administered drug because of its large surface area (Artursson *et al.* 2007; Pires *et al.* 2015). Sesamin, asarinin, (–)-epicatechin, (+)-catechin, and quercetin were predicted to be highly absorbed in the human intestines, while the rest are poorly absorbed.

Skin permeability is important in the development of transdermal drug delivery systems and other topical drug formulations (Pires *et al.* 2015; Supe and Takudage 2021). The more negative the log Kp, with Kp in cm/s, the lesser the ability of the compound to pass through the skin (Daina *et al.* 2017). Thus, stigmasterol and β -sitosterol are the most skin permeant among the best binding compounds with log Kp values of -2.74 and -2.2 , respectively.

The p-glycoprotein (P-gp) is the most important member of the ATP-binding cassette transporters (Daina *et al.* 2017). It has a vital role in reducing the absorption of xenobiotics, such as drugs, and toxins by extruding these compounds and protecting the cells against toxicity. This is also the cause of the resistance of cancer cells to chemotherapeutic agents (Wolf and Paine 2018). Due to its influence on the ADMET properties of compounds, prediction of

Table 2. Predicted ADMET properties from pkCSM and SwissADME.

ADMET properties	Active compounds					
	Sesamin	Asarinin	Quercetin-7-rutinoside	Kaempferol-3-rutinoside	(-)-Epicatechin	(+)-Catechin
Water solubility – ESOL class	Soluble	Soluble	Soluble	Soluble	Soluble	Soluble
Caco2 permeability (log Papp in 10 ⁻⁶ cm/s)	1.399	1.399	-1.599	0.189	-0.283	-0.283
Intestinal absorption in human	High	High	Low	Low	High	High
Skin permeability – log Kp (cm/s)	-6.56	-6.56	-10.26	-9.91	-7.82	-7.82
P-glycoprotein substrate	No	No	Yes	Yes	Yes	Yes
P-glycoprotein I inhibitor	Yes	Yes	No	No	No	No
P-glycoprotein II inhibitor	No	No	No	No	No	No
VDss in human (log L/kg)	-0.17	-0.17	1.84	1.71	1.027	1.027
Fraction unbound in human (Fu)	0	0	0.165	0.157	0.235	0.235
BBB permeability (log BB)	-0.862	-0.862	-2.056	-1.669	-1.054	-1.054
CNS permeability (log PS)	-2.939	-2.939	-5.07	-5.015	-3.298	-3.298
CYP2D6 substrate	No	No	No	No	No	No
CYP3A4 substrate	Yes	Yes	No	No	No	No
CYP1A2 inhibitor	Yes ^a ; No ^b	Yes ^a ; No ^b	No ^a ; No ^b	No ^a ; No ^b	No ^a ; No ^b	No ^a ; No ^b
CYP2C19 inhibitor	Yes ^a ; Yes ^b	Yes ^a ; Yes ^b	No ^a ; No ^b	No ^a ; No ^b	No ^a ; No ^b	No ^a ; No ^b
CYP2C9 inhibitor	Yes ^a ; No ^b	Yes ^a ; No ^b	No ^a ; No ^b	No ^a ; No ^b	No ^a ; No ^b	No ^a ; No ^b
CYP2D6 inhibitor	No ^a ; Yes ^b	No ^a ; Yes ^b	No ^a ; No ^b	No ^a ; No ^b	No ^a ; No ^b	No ^a ; No ^b
CYP3A4 inhibitor	Yes ^a ; Yes ^b	Yes ^a ; Yes ^b	No ^a ; No ^b	No ^a ; No ^b	No ^a ; No ^b	No ^a ; No ^b
Total clearance (log ml/min/kg)	-0.126	-0.126	-0.387	-0.16	0.183	0.183
Renal OCT2 substrate	No	No	No	No	No	No
Ames toxicity	Yes	Yes	No	No	No	No
Max. tolerated dose in human (log mg/kg/d)	0.089	0.089	0.461	0.481	0.438	0.438
hERG I inhibitor	No	No	No	No	No	No
hERG II inhibitor	No	No	Yes	Yes	No	No
Oral rat acute toxicity – LD50 (mol/kg)	2.883	2.883	2.501	2.513	2.428	2.428
Oral rat chronic toxicity – LOAEL (log mg/kg_bw/d)	1.568	1.568	3.667	3.569	2.5	2.5
Hepatotoxicity	No	No	No	No	No	No
Skin sensitization	No	No	No	No	No	No

ESOL – estimated solubility; Papp – apparent permeability; VDss – steady-state volume of distribution; BBB – blood-brain barrier; CNS – central nervous system; OCT2 – organic cation transporter 2; hERG – human ether-a-go-go-related gene; LD50 – median lethal dose; LOAEL – lowest observed adverse effect level

^apkCSM

^bSwissADME

the possibility of a compound to be a substrate or an inhibitor of P-gp is important in the early phase of the drug discovery (Montanari and Ecker 2015). Quercetin-7-rutinoside, kaempferol-3-rutinoside, (-)-epicatechin, (+)-catechin, myricetin-3-rutinoside, quercetin, and kaempferol-3-rhamnoside-7-glucoside were predicted to be P-gp substrates. On the other hand, sesamin and asarinin are inhibitors of P-gp I, and stigmaterol, and β -sitosterol were inhibitors of both P-gp I and II.

Distribution. The steady-state volume of distribution or VDss is an important pharmacokinetic parameter needed for the design of a suitable drug dosage regimen (Zhivkova

et al. 2015). It is the volume of plasma or blood in which the compound appears to be dissolved at a steady state or equilibrium (Freitas *et al.* 2015). VDss is considered as low if log L/kg is lower than -0.15 and high if it is higher than 0.45. The higher the volume of distribution, the more a compound is distributed in tissue than in plasma (Pires *et al.* 2015). All best binding compounds have high VDss except sesamin and asarinin that both have -0.17, which means that they are more distributed in plasma than in the tissue.

The unbound fraction of a compound is the portion that exerts a therapeutic or pharmacologic effect because it is not bound to plasma proteins (Heuberger *et al.* 2013).

Table 2 (continued). Predicted ADMET properties from pkCSM and SwissADME.

ADMET properties	Active compounds				
	Myricetin-3-rutinoside	Quercetin	Kaempferol 3-rhamnoside-7-glucoside	Stigmasterol	β -Sitosterol
Water solubility – ESOL class	Soluble	Soluble	Soluble	Poorly soluble	Poorly soluble
Caco2 permeability (log Papp in 10 ⁻⁶ cm/s)	-1.138	-0.229	-0.771	1.213	1.201
Intestinal absorption in human	Low	High	Low	Low	Low
Skin permeability – log Kp (cm/s)	-10.61	-7.05	-10.35	-2.74	-2.2
P-glycoprotein substrate	Yes	Yes	Yes	Yes	No
P-glycoprotein I inhibitor	No	No	No	Yes	Yes
P-glycoprotein II inhibitor	No	No	No	0.178	Yes
VDss in human (log L/kg)	1.271	1.559	1.261	0	0.193
Fraction unbound in human (Fu)	0.223	0.206	0.181	0.771	0
BBB permeability (log BB)	-2.215	-1.098	-1.957	-1.652	0.781
CNS permeability (log PS)	-5.397	-3.065	-5.066	No	-1.705
CYP2D6 substrate	No	No	No	Yes	No
CYP3A4 substrate	No	No	No	Yes	Yes
CYP1A2 inhibitor	No ^a ; No ^b	Yes ^a ; Yes ^b	No ^a ; No ^b	No ^a ; No ^b	No ^a ; No ^b
CYP2C19 inhibitor	No ^a ; No ^b	No ^a ; No ^b	No ^a ; No ^b	No ^a ; No ^b	No ^a ; No ^b
CYP2C9 inhibitor	No ^a ; No ^b	No ^a ; No ^b	No ^a ; No ^b	No ^a ; Yes ^b	No ^a ; No ^b
CYP2D6 inhibitor	No ^a ; No ^b	No ^a ; Yes ^b	No ^a ; No ^b	No ^a ; No ^b	No ^a ; No ^b
CYP3A4 inhibitor	No ^a ; No ^b	No ^a ; Yes ^b	No ^a ; No ^b	No ^a ; No ^b	No ^a ; No ^b
Total clearance (log mL/min/kg)	-0.513	0.407	-0.046	0.618	0.628
Renal OCT2 substrate	No	No	No	No	No
Ames toxicity	No	No	No	No	No
Max. tolerated dose in human (log mg/kg/d)	0.441	0.499	0.504	-0.664	-0.621
hERG I inhibitor	No	No	No	No	No
hERG II inhibitor	Yes	No	Yes	Yes	Yes
Oral rat acute toxicity – LD50 (mol/kg)	2.484	2.471	2.562	2.54	2.552
Oral rat chronic toxicity – LOAEL (log mg/kg_bw/d)	3.919	2.612	4.76	0.872	0.855
Hepatotoxicity	No	No	No	No	No
Skin sensitization	No	No	No	No	No

ESOL – estimated solubility; Papp – apparent permeability; VDss – steady-state volume of distribution; BBB – blood-brain barrier; CNS – central nervous system; OCT2 – organic cation transporter 2; hERG – human ether-a-go-go-related gene; LD50 – median lethal dose; LOAEL – lowest observed adverse effect level

^apkCSM

^bSwissADME

Sesamin, asarinin, stigmasterol, and β -sitosterol were found to have zero unbound fraction. This means that they are highly bound to proteins and may not exert a good pharmacologic effect.

Predicting the ability of a compound to cross the blood-brain barrier (BBB) helps to reduce toxicities or side effects of lead compounds. It can also help in improving the efficacy of drugs that exerts pharmacologic activity in the brain. Compounds with log BB higher than 0.3 can readily cross the BBB, while compounds with log BB lower than -1 are poorly distributed to the brain (Pires *et al.* 2015). The compounds that were predicted to readily cross the BBB are stigmasterol and β -sitosterol.

The blood-brain permeability–surface area product (log PS) is a more direct measurement than the BBB permeability measurement since this is generated from *in situ* brain perfusions with the compound directly injected

into the carotid artery. This method is free from systemic distribution effects which may distort brain permeation. Compounds with a log PS or higher than -2 can penetrate the central nervous system or CNS, while those with lower than -3 are unable to penetrate CNS (Suenderhauf *et al.* 2012; Pires *et al.* 2015). Only stigmasterol and β -sitosterol were predicted to have the ability to penetrate CNS, which means that they may exert pharmacologic activity or induce side effects in the CNS.

Metabolism. The cytochrome P450 (CYP450) enzymes are responsible for about 95% of the metabolism of drugs in the market (Xu *et al.* 2012). The CYP450 isoforms responsible for 90% of drug metabolism are CYP1A2, CYP2C9, CYP2C99, CYP2D6, and CYP3A4 (Cheng *et al.* 2011). CYP450 can dramatically alter the ADMET of compounds. Thus, it is important to evaluate if a compound is a substrate or an inhibitor of these enzymes (Pires *et al.* 2015). Substrates are compounds that bind

to the active site of an enzyme and are transformed to metabolites, which are either inactive form for clearance or active form if the compound is a prodrug, while they are in the active site (Deodhar *et al.* 2020; Zanger and Schwab 2013). The predicted CYP3A4 substrates are sesamin, asarinin, stigmaterol, and β -sitosterol, which means that they are metabolized when they bind to CYP3A4. Inhibitors are compounds that bind to or block the substrate's binding site, which modify the enzyme's catalytic property (Gomes and Rocha-Santos 2019). Sesamin and asarinin were expected to be inhibitors of all the five CYP450 enzymes. Stigmaterol was predicted to inhibit CYP2C9. Quercetin was also predicted to be a CYP1A2, CYP2D6, and CYP3A4 inhibitor. These compounds may cause drug-drug interactions when taken with drugs or prodrugs that are metabolized by the said enzymes. The drug-drug interaction may result in a decrease in clearance of the drug, which may lead to toxicity, or reduce the pharmacologic effect of a prodrug that needs to be metabolized to be activated.

Excretion. Total clearance is the combination of hepatic and renal clearances and is related to bioavailability. It is important in determining rates of dosing to achieve steady-state concentrations. The predicted total clearance of the compounds is given in log mL/min/kg (Pires *et al.* 2015). β -sitosterol and stigmaterol were predicted to have the highest total clearance, 0.628 and 0.618, respectively. This means that they are more rapidly removed from the body.

Approximately 40% of drugs in the market are cationic (Belzer *et al.* 2013). The renal organic cation transporter 2 (OCT2) is important in the renal excretion of cationic drugs. This raises a risk of drug interactions, especially in compounds that inhibit this transporter, which decrease the clearance of OCT2 substrate (Hacker *et al.* 2015). None of the best binding compounds were predicted to be renal OCT2 substrates.

Toxicity. AMES test uses bacteria to assess the mutagenicity potential of a compound (Pires *et al.* 2015). The detection of the mutagenicity potential of a compound in the early stages of drug discovery could help to stop the development of harmful drugs (Hsu *et al.* 2016). Sesamin and asarinin were predicted to be mutagenic. Thus, they may act as carcinogens.

The maximum tolerated dose (MTD) provides an estimate of the toxic threshold dose of a compound in humans. This information is important in the determination of the maximum recommended starting dose of a drug. An MTD of less than or equal to 0.477 log mg/kg/d is considered low, while a value greater than 0.477 log mg/kg/d is high (Pires *et al.* 2015). Kaempferol-3-rutinoside, quercetin, and kaempferol-3-rhamnoside-7-glucoside were predicted to have high MTD – which were 0.481, 0.499, and 0.504

log mg/kg/d. This means that these are the highest doses that humans can tolerate without experiencing the toxic effect of the compounds.

The inhibition of the human ether-a-go-go-related gene (hERG) that encodes potassium channels may lead to QT interval prolongation and eventually, *torsades de pointes* or ventricular tachycardia, and even death. To avoid these serious adverse effects, prediction of a drug candidate's ability to inhibit hERG is essential (Pires *et al.* 2015; Hanser *et al.* 2019). Quercetin-7-rutinoside, kaempferol-3-rutinoside, myricetin-3-rutinoside, kaempferol-3-rhamnoside-7-glucoside, stigmaterol, and β -sitosterol were predicted to inhibit hERG II.

The median lethal dose or (LD50) is used to measure acute toxicity in rats, which assesses the relative toxicity of a compound (Pires *et al.* 2015). The lower the LD50, the more lethal the compound is. The LD50 values of the best binding compounds were found to be near to each other. (-)-Epicatechin and (+)-catechin have the lowest predicted LD50 (2.428 mol/kg), which means that they are the most lethal among the best binding compounds. On the other hand, sesamin and asarinin have the highest predicted LD50 (2.883 mol/kg), which means that they are the least lethal among the best binding compounds.

Oral rat chronic toxicity testing gives information on the possible unpleasant adverse effects that may arise from repeated exposure to a compound over a long period of time (OECD 2018). It identifies the lowest dose of a compound that results in an observed adverse effect, which is called the lowest observed adverse effect level or LOAEL in log mg/kg body weight (bw)/d (Pires *et al.* 2015). β -Sitosterol and stigmaterol were predicted to have the lowest dose that can cause adverse effects, which are 0.855 and 0.872 log mg/kg_bw/d, respectively.

Liver toxicity caused by drugs is a pressing safety concern during drug development and ranks among the top reasons for drug attrition (Pires *et al.* 2015; Mulliner *et al.* 2016). Skin sensitization, resulting in allergic contact dermatitis, is another drug-induced problem that can trigger life-threatening health conditions (Chong *et al.* 2018). None of the best binding compounds were predicted to cause hepatotoxicity and skin sensitization.

Drug-likeness. qualitatively evaluates the chance for a compound to become an oral drug with respect to its bioavailability (Daina *et al.* 2017). It assesses the resemblance of a compound to existing drugs (Athar *et al.* 2019). The SwissADME drug-likeness section is composed of five different rule-based filters: the Lipinski (which is the pioneer of rule-of-five), Ghose, Veber, Egan, and Muegge. SwissADME utilizes the Abbott bioavailability score, which relies on the total charge, topological polar surface area, and violation of compounds

Table 3. Drug-likeness of the best binding compounds.

Active compounds	Lipinski	Ghose	Veber	Egan	Muegge	Bioavailability score
Sesamin	Yes	Yes	Yes	Yes	Yes	0.55
Asarinin	Yes	Yes	Yes	Yes	Yes	0.55
Quercetin-7-rutinoside	No	No	No	No	No	0.17
Kaempferol-3-rutinoside	No	No	No	No	No	0.17
(-)-Epicatechin	Yes	Yes	Yes	Yes	Yes	0.55
(+)-Catechin	Yes	Yes	Yes	Yes	Yes	0.55
Myricetin-3-rutinoside	No	No	No	No	No	0.17
Quercetin	Yes	Yes	Yes	Yes	Yes	0.55
Kaempferol 3-rhamnoside-7-glucoside	No	No	No	No	No	0.17
Stigmasterol	Yes	No	Yes	No	No	0.55
β -Sitosterol	Yes	No	Yes	No	No	0.55

to the Lipinski filter. It predicts the probability of a compound to have at least 10% oral bioavailability in rats or measurable Caco-2 permeability. The bioavailability score also identifies the poorly- and well-absorbed compounds (Martin 2005; Daina *et al.* 2017).

The predicted drug-likeness of the best binding compounds are shown in Table 3. Only sesamin, asarinin, (-)-epicatechin, (+)-catechin, and quercetin satisfied all the five drug-likeness filters. They have a bioavailability score of 0.55 along with stigmasterol and β -sitosterol, which passed the Lipinski and Veber filters. On the other hand, quercetin-7-rutinoside, kaempferol-3-rutinoside, myricetin-3-rutinoside, and kaempferol 3-rhamnoside-7-glucoside violated all the five drug-likeness filters; they have a bioavailability score of 0.17. A bioavailability score of 0.55 signifies the compounds that passed the rule-of-five and 0.17 for those that failed. The compounds with a bioavailability score of 0.55 are more well-absorbed compared to those that have 0.17.

CONCLUSION

CADD methods are essential for the preliminary stage of drug discovery. The molecular docking simulation allowed the investigation of the behavior of compounds from *M. acuminata* Colla peel in the binding site of human intestinal α -glucosidase. Compounds that have a better or comparable inhibitory activity to the standard, acarbose, against α -glucosidase were determined – namely, sesamin, asarinin, quercetin-7-rutinoside, kaempferol-3-rutinoside, (-)-epicatechin, (+)-catechin, myricetin-3-rutinoside, quercetin, kaempferol-3-rhamnoside-7-glucoside, stigmasterol, and β -sitosterol. The prediction of ADMET properties and drug-likeness revealed how

these best binding compounds may behave inside the body. (-)-Epicatechin, (+)-catechin, and quercetin were found to be safe and have good absorption, distribution, metabolism (except quercetin), and excretion properties. They passed all the five drug-likeness filters. The promising potentials showed by (-)-epicatechin, (+)-catechin, and quercetin in the molecular docking and their ADMET properties may direct them for consideration as lead compounds that may be developed into drugs. Thus, the conduct of *in vitro* and *in vivo* laboratory experiments for the confirmation of the α -glucosidase inhibitory activity and ADMET properties of (-)-epicatechin, (+)-catechin, and quercetin from *M. acuminata* Colla peel is recommended.

ACKNOWLEDGMENTS

This study was funded under the Accelerated Science and Technology Human Resource Development Program of the Department of Science and Technology and the University of the Philippines Manila–National Institutes of Health Student/Thesis Research Grant. The valuable contributions of Dr. Isidro C. Sia, Dr. Bienvenido S. Balotro, Prof. Teresita S. de Guzman, Prof. Shiela May J. Nacabu-an, and Dr. Junie B. Billones to this study are greatly acknowledged. The authors are grateful to the developers of all the computational tools used and to the rest of the people who helped in this study.

NOTES ON APPENDICES

The complete appendices section of the study is accessible at <http://philjournsci.dost.gov.ph>

REFERENCES

- ABDULKHALEQLA, ASSIMA, NOOR M, ABDULLAH R, SAAD MZ, TAUFIQ-YAP YH. 2017. Therapeutic uses of epicatechin in diabetes and cancer. *Veterinary World* 10(8): 869–872.
- ABELIANA, DYBEKM, WALLACHJ, GAYEB, ADEJARE A. 2021. Pharmaceutical chemistry. In: Remington: The Science and Practice of Pharmacy, Twenty-third Edition. Adejare A ed. Amsterdam: Elsevier. p. 105–128.
- [ADA] American Diabetes Association. 2011. Diagnosis and classification of diabetes mellitus. *Diabetes Care* 34(1): S62–S69.
- ANTHONY J, RANGAMARAN VR, SHIVASANKARASUBBIAH KT, GOPAL D, RAMALINGAM K. 2016. Applications of molecular docking: Its impact and importance outside the purview of drug discovery. In: Applied Case Studies and Solutions in Molecular Docking-based Drug Design. Dastmalchi S, Hamzeh-Mivehroud M, Sokouti B eds. Pennsylvania: IGI Global. p. 278–306.
- ARTURSSON P, NEUHOF S, MATSSON P, TAVELIN S. 2007. Passive permeability and active transport models for the prediction of oral absorption. In: Comprehensive Medicinal Chemistry II, Vol. 5. Taylor JB, Triggle DJ eds. Amsterdam: Elsevier. p. 259–278.
- ATHAR M, SONAAN, BEKONO BD, NTIE-KANG F. 2019. Fundamental physical and chemical concepts behind “drug-likeness” and “natural product-likeness”. *Physical Sciences Reviews* 4: 20180101.
- BARROSO WA, ABREU IC, RIBEIRO LS, DA ROCHA CQ, DE SOUZA HP, DE LIMA TM. 2019. Chemical composition and cytotoxic screening of *Musa cavendish* green peels extract: antiproliferative activity by activation of different cellular death types. *Toxicology In Vitro* 59: 179–186.
- BELL EW, ZHANG Y. 2019. DockRMSD: an open-source tool for atom mapping and RMSD calculation of symmetric molecules through graph isomorphism. *J Cheminform* 11(1): 40.
- BELZER M, MORALES M, JAGADISH B, MASH EA, WRIGHT SH. 2013. Substrate-dependent ligand inhibition of the human organic cation transporter OCT2. *The Journal of Pharmacology and Experimental Therapeutics* 346(2): 300–310.
- BHARATHKUMAR H, SUNDARAM MS, JAGADISH S, PARICHARAK S, HEMSHEKHAR M, MASON D, KEMPARAJU K, GIRIS KS, BASAPPA, BENDER A, RANGAPPA KS. 2014. Novel benzoxazine-based aglycones block glucose uptake *in vivo* by inhibiting glycosidases. *PLoS One* 9(7): e102759.
- CHENG F, YU Y, ZHOU Y, SHEN Z, XIAO W, LIU G, LI W, LEE PW, TANG Y. 2011. Insights into molecular basis of cytochrome P450 inhibitory promiscuity of compounds. *Journal of Chemical Information and Modeling* 51(10): 2482–2495.
- CHONG LH, LI H, WETZEL I, CHO H, TOH Y. 2018. A liver-immune coculture array for predicting systemic drug-induced skin sensitization. *Lab on a Chip* 18(21): 3239–3250.
- CHUKWUEMEKA PO, UMAR HI, IWALOYE O, ORETADE OM, OLOWOSOKO CB, ELABIYI MO, IGBE FO, ORETADE OJ, EIGBE JO, ADEOJO FJ. 2021. Targeting p53-MDM2 interactions to identify small molecule inhibitors for cancer therapy: beyond “failure to rescue”. *Journal of Biomolecular Structure & Dynamics*. p. 1–19.
- DAINAA, MICHELINO, ZOETE V. 2017. SwissADME: a free web tool to evaluate pharmacokinetics, drug-likeness and medicinal chemistry friendliness of small molecules. *Sci Rep* 7: 42717.
- DALLAKYAN S, OLSON AJ. 2015. Small-molecule library screening by docking with PyRx. *Methods in Molecular Biology* 1263: 243–250.
- DARAM, MIR S. 2017. Molecular docking: Approaches, types, applications and basic challenges. *J Anal Bioanal Tech* 8: 356.
- DEODHAR M, AL RIHANI SB, ARWOOD MJ, DARAKJIAN L, DOW P, TURGEON J, MICHAUD V. 2020. Mechanisms of CYP450 inhibition: understanding drug-drug interactions due to mechanism-based inhibition in clinical practice. *Pharmaceutics* 12(9): 846.
- DHORAJIWALA TM, HALDER ST, SAMANT L. 2019. Comparative *In silico* molecular docking analysis of L-threonine-3-dehydrogenase, a protein target against African trypanosomiasis using selected phytochemicals. *J Appl Biotechnol Rep* 6(3): 101–108.
- DURÁN-ITURBIDE NA, DÍAZ-EUFRACIO BI, MEDINA-FRANCO JL. 2020. *In silico* ADME/Tox profiling of natural products: a focus on BIOFACQUIM. *ACS Omega* 5(26): 16076–16084.
- ETSASSALANGER, BADMUS JA, MARNEWICK JL, IWUOHA EI, NCHU F, HUSSEIN AA. 2020. Alpha-glucosidase and alpha-amylase inhibitory activities, molecular docking, and antioxidant capacities of *Salvia aurita* constituents. *Antioxidants* 9(11): 1149.
- FREITAS AA, LIMBU K, GHAFOURIAN T. 2015. Predicting volume of distribution with decision tree-based regression methods using predicted tissue: plasma partition coefficients. *J Cheminform* 7(6): 1–17.

- GOMES AR, ROCHA-SANTOS TAP. 2019. Bioassay: Enzyme Assay. In Encyclopedia of Analytical Science Third Edition. Worsfold P, Poole C, Townshend A, Miró M eds. Amsterdam: Elsevier. p. 271–277.
- GONZÁLEZ-MONTELONGO R, LOBO MG, GONZÁLEZ M. 2010. Antioxidant activity in banana peel extracts: testing extraction conditions and related bioactive compounds. Food Chemistry 119: 1030–1039.
- HABTEMARIAM S. 2011. A-glucosidase inhibitory activity of kaempferol-3-O-rutinoside. Natural Product Communications 6(2): 201–203.
- HACKER K, MAAS R, KORNHUBER J, FROMM MF, ZOLK O. 2015. Substrate-dependent inhibition of the human organic cation transporter OCT2: a comparison of metformin with experimental substrates. PLoS One 10(9): e0136451.
- HAJALSIDDIG T, OSMAN A, SAEED A. 2020. 2D-QSAR modeling and molecular docking studies on 1*H*-Pyrazole-1-carbothioamide derivatives as EGFR kinase inhibitors. ACS Omega 5(30): 18662–18674.
- HANSER T, STEINMETZ F, PLANTE J, RIPPMMANN F, KRIER M. 2019. Avoiding hERG-liability in drug design *via* synergetic combinations of different (Q) SAR methodologies and data sources: a case study in an industrial setting. Journal of Cheminformatics 11(1): 9.
- HEUBERGER J, SCHMIDT S, DERENDORF H. 2013. When is protein binding important? Journal of Pharmaceutical Sciences 102(9): 3458–3467.
- HSU PF, SUNG SH, CHENG HM, SHIN SJ, LIN KD, CHONG K, YEN FS, YU BH, HUANG CT, HSU CC. 2018. Cardiovascular benefits of acarbose *vs.* sulfonylureas in patients with type 2 diabetes treated with metformin. The Journal of Clinical Endocrinology and Metabolism 103(10): 3611–3619.
- JIANG J, ZHAO L, LIN L, GUI M, ALETENG Q, WU B, WANG S, PAN B, LING Y, GAO X. 2017. Postprandial blood glucose outweighs fasting blood glucose and HbA1c in screening coronary heart disease. Scientific Reports 7(1): 14212.
- JOSHI SR, STANDL E, TONG N, SHAH P, KALRA S, RATHOD R. 2015. Therapeutic potential of a-glucosidase inhibitors in type 2 diabetes mellitus: an evidence-based review. Expert Opin Pharmacother 16(13): 1959–1981.
- KOSTAL J. 2016. Computational chemistry in predictive toxicology: *status quo et quo vadis?* In: Advances in Molecular Toxicology, Vol. 10. Fishbein JC, Heilman JM eds. Amsterdam: Elsevier. p. 139–186.
- LEELANANDA SP, LINDERT S. 2016. Computational methods in drug discovery. Beilstein Journal of Organic Chemistry 12: 2694–2718.
- MACALINO SJY, GOSU V, HONG S, CHOI S. 2015. Role of computer-aided drug design in modern drug discovery. Archives of Pharmacal Research 38(9): 1686–1701.
- MARTIN YC. 2005. A bioavailability score. Journal of Medicinal Chemistry 48(9): 3164–3170.
- MATHEW NS, NEGI PS. 2016. Traditional uses, phytochemistry and pharmacology of wild banana (*Musa acuminata* Colla): a review. Journal of Ethnopharmacology 196: 124–140.
- MOKBEL MS, HASHINAGA F. 2005. Antibacterial and antioxidant activities of banana (*Musa*, AAA cv. Cavendish) fruits peel. American Journal of Biochemistry and Biotechnology 1(3): 125–131.
- MONTANARI F, ECKER GF. 2015. Prediction of drug-ABC-transporter interaction—recent advances and future challenges. Advanced Drug Delivery Reviews 86: 17–26.
- MOOTOOSAMY A, MAHOMOODALLY MF. 2013. Ethnomedicinal application of native remedies used against diabetes and related complications in Mauritius. Journal of Ethnopharmacology 151: 413–444.
- MORDI RC, FADIARO AE, OWOEYE TF, OLANREWaju IO, UZOAMAKA GC, OLORUNSHOLA SJ. 2016. Identification by GC-MS of the components of oils of banana peels extract, phytochemical and antimicrobial analyses. Research Journal of Phytochemistry 10: 39–44.
- MULLINER D, SCHMIDT F, STOLTE M, SPIRKL HP, CZICH A, AMBERG A. 2016. Computational models for human and animal hepatotoxicity with a global application scope. Chemical Research in Toxicology 29(5): 757–767.
- MURUGESU S, IBRAHIM Z, AHMED Q, YUSOFF NI, UZIR B, PERUMAL V, ABAS F, SAARI K, EL-SEEDI H, KHATIB A. 2018. Characterization of α -glucosidase inhibitors from *Clinacanthus nutans* Lindau leaves by gas chromatography–mass spectrometry-based metabolomics and molecular docking simulation. Molecules 23(9): 2402.
- NAVGHARE VV, DHAWALE SC. 2016. *In vitro* antioxidant, hypoglycemic and oral glucose tolerance test of banana peels. Alexandria Journal of Medicine 53: 237–243.
- NAVGHARE V, DHAWALE S, PHANSE M. 2019. Assessment of antidiabetic potential of *Musa acuminata*

- peel extract and its fractions in experimental animals and characterisation of its bioactive compounds by HPTLC. Archives of Physiology and Biochemistry. p. 1–13.
- NEILSON AP, FERRUZZI MG. 2011. Influence of formulation and processing on absorption and metabolism of flavan-3-ols from tea and cocoa. Annual Review of Food Science and Technology 2: 125–151.
- NIAMAH AK. 2015. Determination, identification of bioactive compounds extracts from yellow banana peels and used *in vitro* as antimicrobial. International Journal of Phytomedicine 6(4): 625–632.
- O'BOYLE NM, BANCK M, JAMES CA, MORLEY C, VANDERMEERSCH T, HUTCHISON GR. 2011. Open Babel: an open chemical toolbox. Journal of Cheminformatics 3: 33.
- [OECD] Organisation for Economic Co-operation and Development. 2018. Test no. 452: chronic toxicity studies. In: OECD Guidelines for the Testing of Chemicals, Section 4. Paris: OECD Publishing.
- OPO F, RAHMAN MM, AHAMMAD F, AHMED I, BHUIYAN MA, ASIRI AM. 2021. Structure based pharmacophore modeling, virtual screening, molecular docking and ADMET approaches for identification of natural anti-cancer agents targeting XIAP protein. Scientific Reports 11(1): 4049.
- OTTAVIANI G, GOSLING DJ, PATISSIER C, RODDE S, ZHOU L, FALLER B. 2010. What is modulating solubility in simulated intestinal fluids? European Journal of Pharmaceutical Sciences 41(3–4): 452–457.
- OU-YANG SS, LU JY, KONG XQ, LIANG ZJ, LUO C, JIANG H. 2012. Computational drug discovery. Acta Pharmacologica Sinica 33(9): 131–1140.
- PADAMBS, TIN HS, CHYE FY, ABDULLAH MI. 2014. Banana by-products: an under-utilized renewable food biomass with great potential. Journal of Food Science and Technology 51(12): 3527–3545.
- PEREIRA DF, CAZAROLLI LH, LAVADO C, MENGATTO V, FIGUEIREDO MS, GUEDES A, PIZZOLATTI MG, SILVA FR. 2011. Effects of flavonoids on α -glucosidase activity: potential targets for glucose homeostasis. Nutrition 27(11–12): 1161–1167.
- PETTERSEN EF, GODDARD TD, HUANG CC, COUCH GS, GREENBLATT DM, MENG EC, FERRIN TE. 2004. UCSF Chimera – a visualization system for exploratory research and analysis. J Comput Chem 25: 1605–1612.
- [PSA] Philippine Statistics Authority. 2021. Registered Deaths in the Philippines, 2019. Retrieved on 25 Jun 2021 from <https://psa.gov.ph/vital-statistics/id/163734>
- PIRESDE, BLUNDELL TL, ASCHER DB. 2015. pkCSM: predicting small-molecule pharmacokinetic and toxicity properties using graph-based signatures. Journal of Medicinal Chemistry 58(9): 4066–4072.
- RAMACHANDRAN S, KOTAP, DING F, DOKHOLYAN NV. 2011. Automated minimization of steric clashes in protein structures. Proteins 79(1): 261–270.
- RAMU R, SHIRAHATTI PS, NAYAKAVADI S, RAMACHANDRAN V, ZAMEER F, DHANANJAYA BL, PRASAD MN N. 2016. The effect of a plant extract enriched in stigmasterol and β -sitosterol on glycaemic status and glucose metabolism in alloxan-induced diabetic rats. Food & Function 7(9): 3999–4011.
- REBELLO LP, RAMOS AM, PERTUZATTI PB, BARCIAMT, CASTILLO-MUÑOZ N, HERMOSÍN-GUTIÉRREZ I. 2014. Flour of banana (*Musa* AAA) peel as a source of antioxidant phenolic compounds. Food Research International 55: 397–403.
- REN L, QIN X, CAO X, WANG L, BAI F, BAI G, SHEN Y. 2011. Structural insight into substrate specificity of human intestinal maltase-glucoamylase. Protein & Cell 2(10): 827–836.
- RENTZSCH R, RENARD BY. 2015. Docking small peptides remains a great challenge: an assessment using AutoDock Vina. Briefings in Bioinformatics 16(6): 1045–1056.
- SAFITRI A, TIRTO SARI D, ROOSDIANA A, FATCHIYAH F. 2020. Molecular docking approach of potential alpha-glucosidase inhibitors from extracts compounds of *R. tuberosa* L. Journal of Smart Bioprospecting and Technology 1(2): 025–030.
- SAMARGHANDIAN S, AZIMI-NEZHAD M, FARKHONDEH T. 2017. Catechin treatment ameliorates diabetes and its complications in streptozotocin-induced diabetic rats. Dose-Response 15(1): 1559325817691158.
- SHANG C, GU Y, KOYAMA T. 2021. Major triterpenes, cycloeucaenone and 31-norcyclolaudenone as inhibitors against both α -glucosidase and α -amylase in banana peel. International Journal of Food Science and Technology 56(7): 3519–3526
- SHAPOVALOV MV, DUNBRACK RL. 2011. A smoothed backbone-dependent rotamer library for proteins derived from adaptive kernel density estimates and regressions. Structure 19(6): 844–858.
- SHENG Z, DAI H, PAN S, WANG H, HU Y, MA W. 2014. Isolation and characterization of an α -glucosidase inhibitor from *Musa* spp. (Baxijiao) flowers. Molecules 19(7): 10563–10573.

- SINGAB AN, YOUSSEF FS, ASHOUR ML. 2014. Medicinal plants with potential antidiabetic activity and their assessment. *Med Aromat Plants* 3(1): 1000151.
- SOMEYAS, YOSHIKI Y, OKUBO K. 2002. Antioxidant compounds from bananas (*Musa Cavendish*). *Food Chemistry* 79: 351–354.
- SUENDERHAUF C, HAMMANN F, HUWYLER J. 2012. Computational prediction of blood-brain barrier permeability using decision tree induction. *Molecules* 17(9): 10429–10445.
- SUPE S, TAKUDAGE P. 2021. Methods for evaluating penetration of drug into the skin: a review. *Skin Research and Technology* 27(3): 299–308.
- [TMIC] The Metabolomics Innovation Centre. 2019a. Showing Compound kaempferol 3-rhamnoside-7-glucoside (FDB093501). Retrieved on 09 Jul 2021 from <https://foodb.ca/compounds/FDB093501>
- [TMIC] The Metabolomics Innovation Centre. 2019b. Showing compound kaempferol 3-rutinoside (FDB016667). Retrieved on 09 Jul 2021 from <https://foodb.ca/compounds/FDB016667>
- [TMIC] The Metabolomics Innovation Centre. 2019c. Showing Compound Myricetin 3-rutinoside (FDB021842). Retrieved on 09 Jul 2021 from <https://foodb.ca/compounds/FDB021842>
- [TMIC] The Metabolomics Innovation Centre. 2019d. Showing compound quercetin 7-rutinoside (FDB017100). Retrieved on 09 Jul 2021 from <https://foodb.ca/compounds/FDB017100>
- TROTT O, OLSON AJ. 2010. AutoDock Vina: improving the speed and accuracy of docking with a new scoring function, efficient optimization, and multithreading. *Journal of Computational Chemistry* 31(2): 455–461.
- VILLAVERDE JJ, OLIVEIRA L, VILELA C, DOMINGUES RM, FREITAS N, CORDEIRO N, FREIRE CSR, SILVERSTRE AJD. 2013. High valuable compounds from the unripe peel of several *Musa* species cultivated in Madeira Island (Portugal). *Ind Crop Prod* 42: 507–512.
- VU HT, SCARLETT CJ, VUONG QV. 2017. Phenolic compounds within banana peel and their potential uses: a review. *Journal of Functional Foods* 40: 238–248.
- WOLF KK, PAINE MF. 2018. Metabolic barrier of the gastrointestinal tract. In: *Comprehensive Toxicology Third Edition*, Vol. 3. McQueen CA ed. Amsterdam: Elsevier. p. 74–98.
- [WHO] World Health Organization. 2016a. Diabetes country profiles, 2016 - Philippines. Retrieved on 21 Jun 2021 from https://www.who.int/diabetes/country-profiles/phl_en.pdf?ua=1
- [WHO] World Health Organization. 2016b. Global report on diabetes. Geneva.
- [WHO] World Health Organization. 2018. Diabetes. Retrieved on 21 Jun 2021 from <https://www.who.int/en/news-room/fact-sheets/detail/diabetes>
- XIANG M, CAO Y, FAN W, CHEN L, MO Y. 2012. Computer-aided drug design: lead discovery and optimization. *Combinatorial Chemistry & High Throughput Screening* 15(4): 328–337.
- XU L, DAS B, PRAKASH C. 2012. CYP450 enzymes in drug discovery and development: an overview. In: *Encyclopedia of Drug Metabolism and Interactions*, First Edition. Lyubimov AV ed. New Jersey: Wiley. p. 1–35.
- ZAINAB B, AYAZ Z, ALWAHIBI MS, KHAN S, RIZWANA H, SOLIMAN DW, ALAWAAD A, MEHMOOD ABBASI A. 2020a. *In silico* elucidation of *Moringa oleifera* phytochemicals against diabetes mellitus. *Saudi Journal of Biological Sciences* 27(9): 2299–2307.
- ZAINAB B, AYAZ Z, MUNIR A, MAHMOUD A, ELSHEIKH MS, MEHMOODA, KHAN S, RIZWAN M, JAHANGIR K, ABBASI A. 2020b. Repositioning of strongly integrated drugs against achromatopsia (CNGB3). *Journal of King Saud University – Science* 32: 1793–1811.
- ZANGER UM, SCHWAB M. 2013. Cytochrome P450 enzymes in drug metabolism: regulation of gene expression, enzyme activities, and impact of genetic variation. *Pharmacology & Therapeutics* 138(1): 103–141.
- ZHIVKOVA ZD, MANDOVA T, DOYTCHINOVA I. 2015. Quantitative structure – pharmacokinetics relationships analysis of basic drugs: volume of distribution. *Journal of Pharmacy & Pharmaceutical Sciences* 18(3): 515–527.

APPENDIX

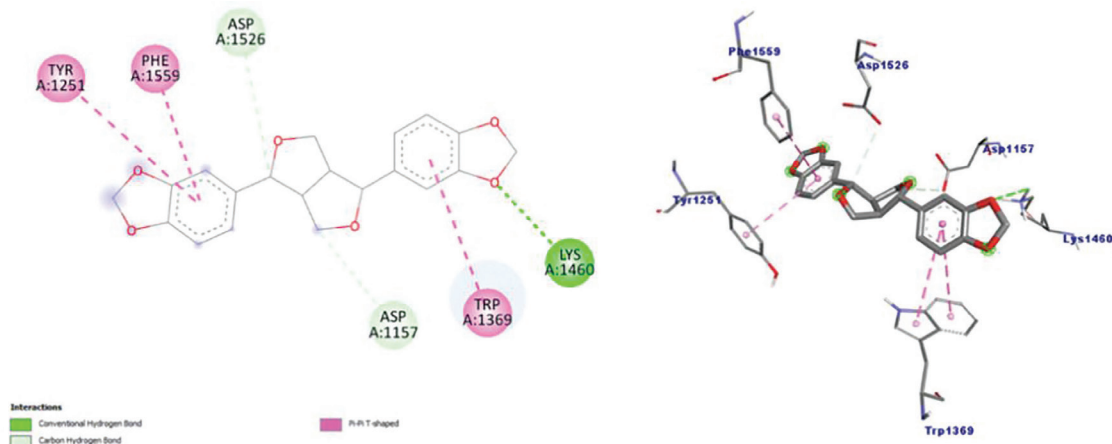


Figure I. 2D and 3D interactions of sesamin with the binding site residues of α -glucosidase.

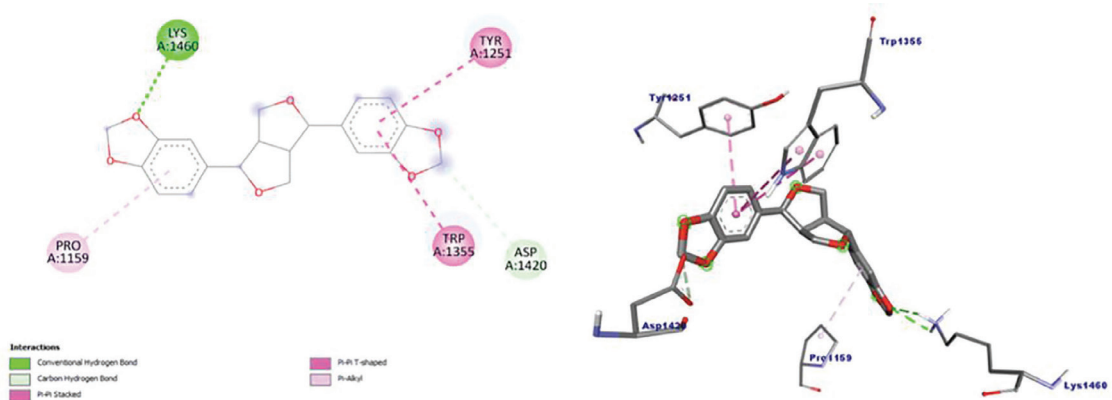


Figure II. 2D and 3D interactions of Asarinin with the binding site residues of α -glucosidase.

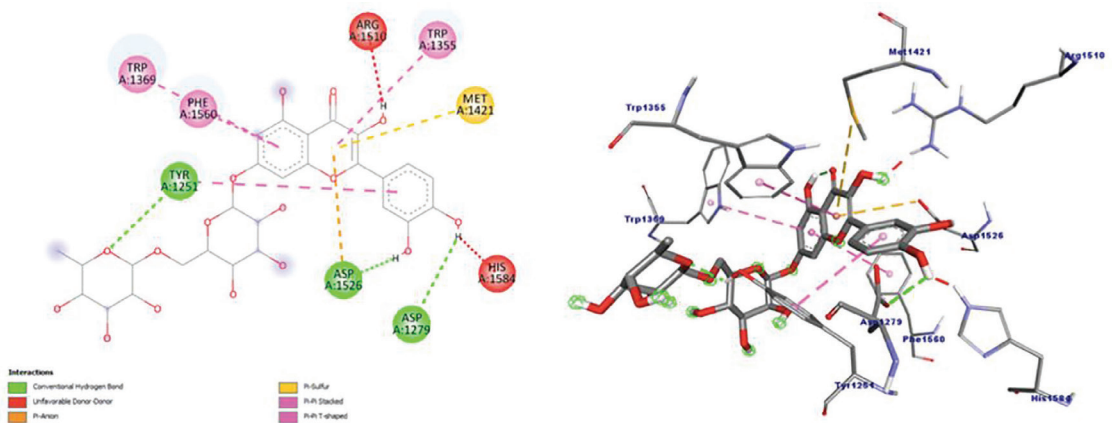


Figure III. 2D and 3D interactions of quercetin-7-rutinoside with the binding site residues of α -glucosidase.

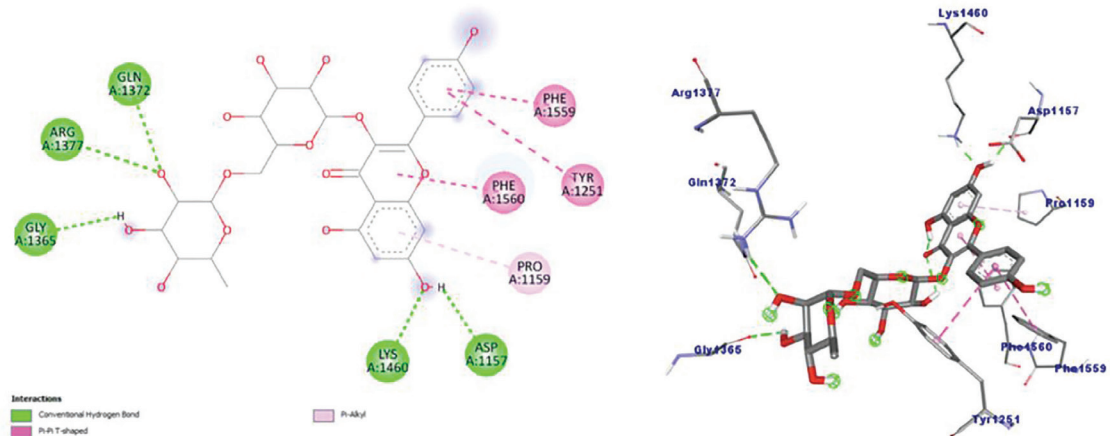


Figure IV. 2D and 3D interactions of kaempferol-3-rutinoside with the binding site residues of α -glucosidase.

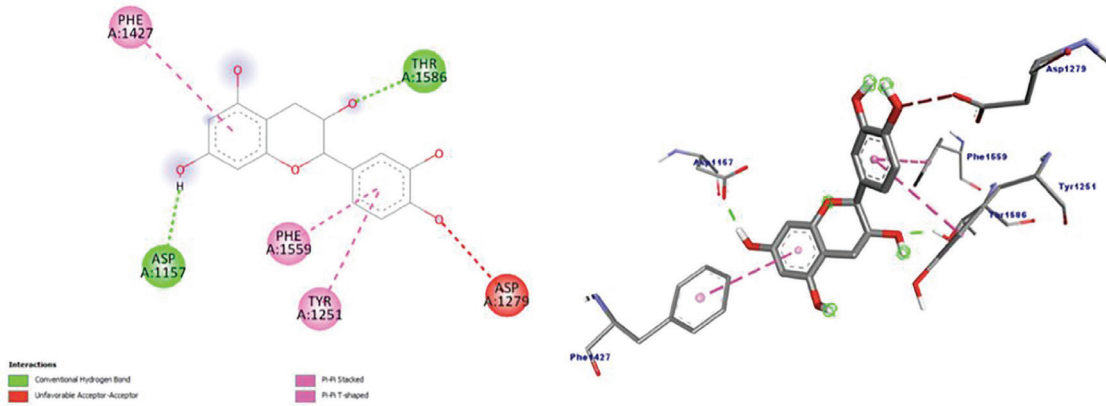


Figure V. 2D and 3D interactions of (-)-epicatechin with the binding site residues of α -glucosidase.

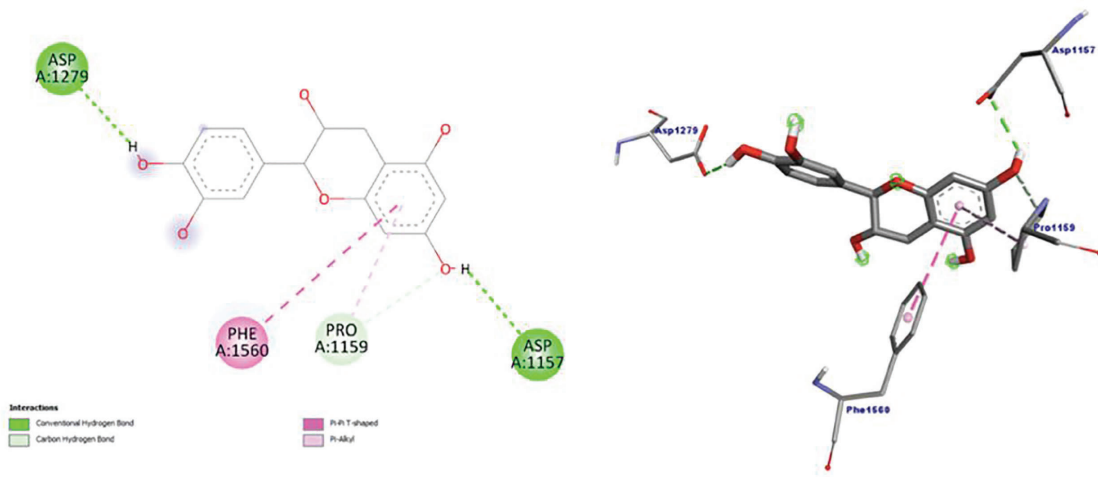


Figure VI. 2D and 3D interactions of (+)-catechin with the binding site residues of α -glucosidase.

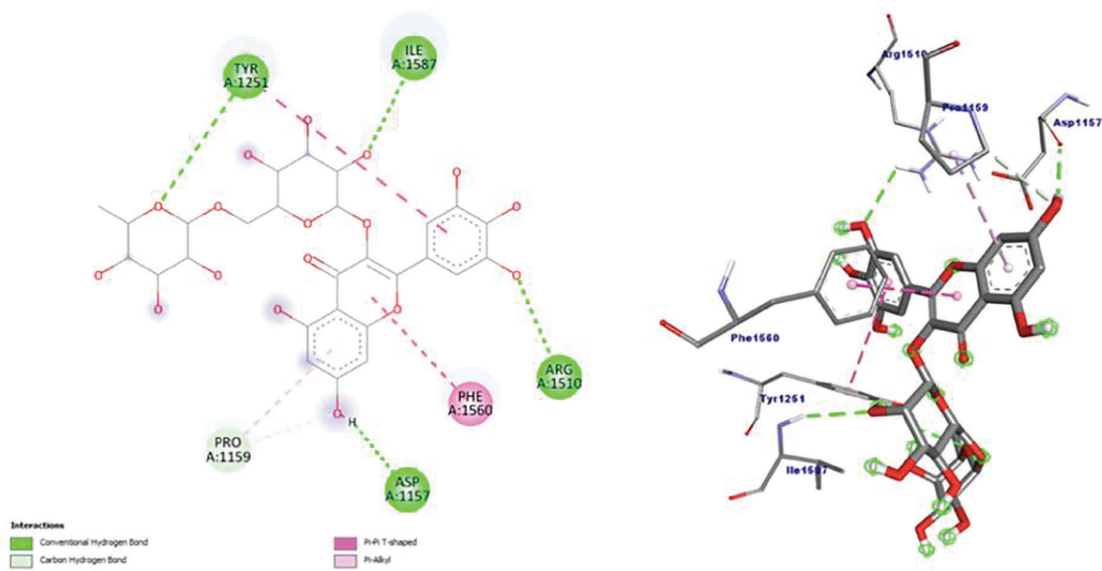


Figure VII. 2D and 3D interactions of myricetin-3-rutinoside with the binding site residues of α -glucosidase.

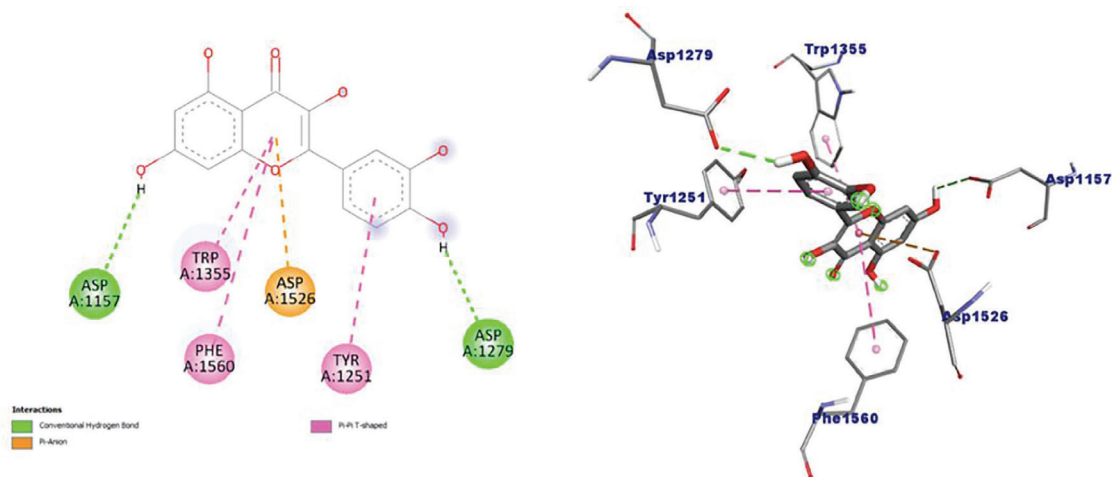


Figure VIII. 2D and 3D interactions of quercetin with the binding site residues of α -glucosidase.

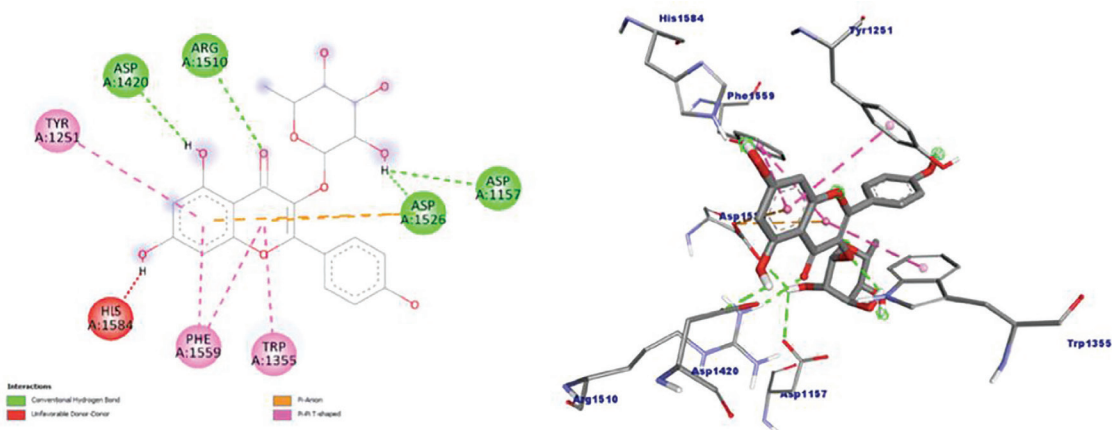


Figure IX. 2D and 3D interactions of kaempferol-3-rhamnoside-7-glucoside with the binding site residues of α -glucosidase.

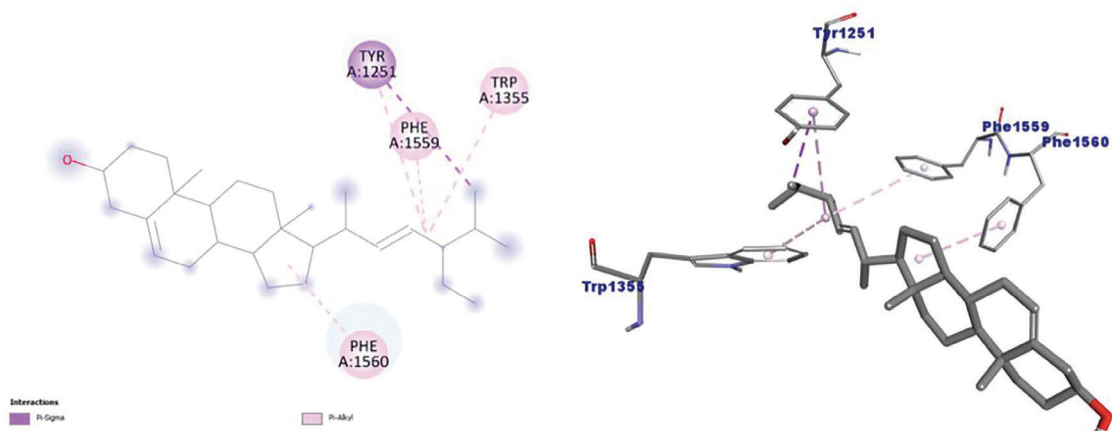


Figure X. 2D and 3D interactions of stigmasterol with the binding site residues of α -glucosidase.

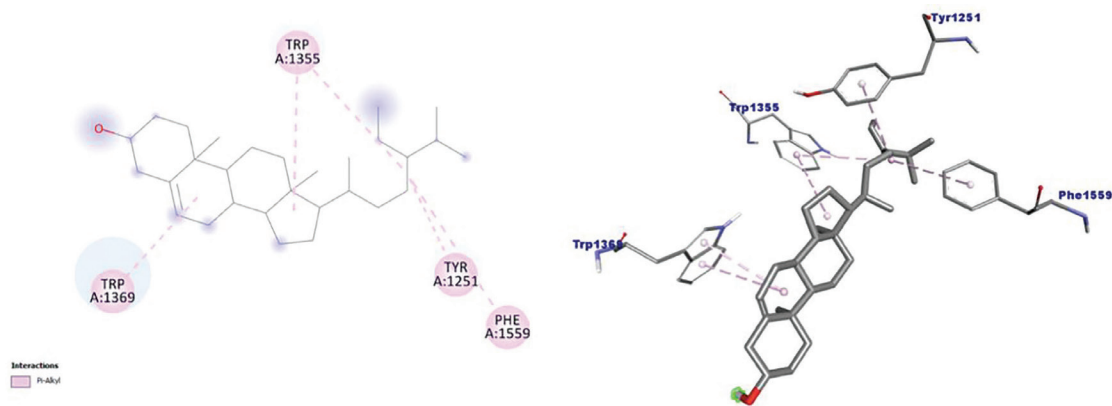

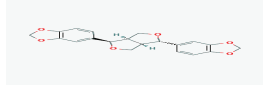
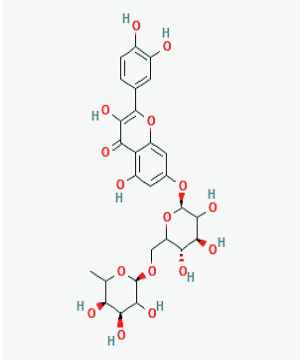
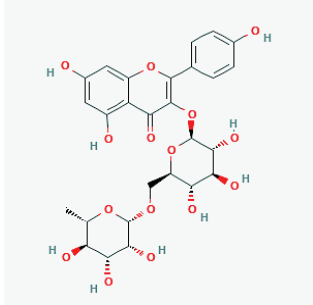
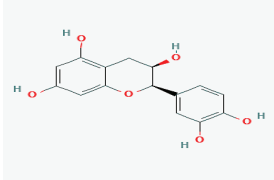
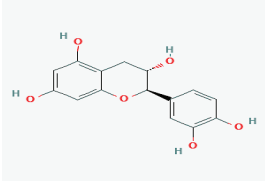


Figure XI. 2D and 3D interactions of β -sitosterol with the binding site residues of α -glucosidase.

Table I. Binding affinities of the 87 compounds from *M. acuminata* Colla peel.

No.	Compound	Binding affinity	No.	Compound	Binding affinity
	Sesamin	-9.8		Decanedioic acid	-6.4
	Asarinin	-9.7		(Z)-octadec-9-en-1-ol	-6.4
	Quercetin-7-rutinoside	-9.4		12-Hydroxystearic acid	-6.4
	Kaempferol-3-rutinoside	-9.4		Octadecanoic acid	-6.3
	(-)-Epicatechin	-9.0		Methyl-9,12-octadecadienoate	-6.3
	Myricetin-3-rutinoside	-8.9		Pentadecanoic acid	-6.3
	(+)-Catechin	-8.9		Heptadecanoic acid	-6.3
	Quercetin	-8.9		Nonadecanoic acid	-6.3
	Stigmasterol	-8.9		Eicosanoic acid	-6.3
	Kaempferol 3-rhamnoside-7-glucoside	-8.9		Hexadec-9-enoic acid	-6.3
	β -Sitosterol	-8.8		22-Hydroxydocosanoic acid	-6.3
	Kaempferol-7-rutinoside	-8.6		Dopamine	-6.3
	Kaempferol-3-rutinoside-7-rhamnoside	-8.7		Benzoic acid	-6.2
	Campesterol	-8.6		Pyrogallol	-6.2
	Isorhamnetin-3-rutinoside	-8.5		Tetradecanoic acid	-6.2
	Procyanidin B2	-8.3		Cis-9-Hexadecenal	-6.2
	31-Norcyclolaudenone	-8.2		2,3-dihydro-3,5-dihydroxy-6-methyl-4H-pyran-4-one	-6.2
	Laricitrin-3-rutinoside	-8.1		Heneicosanoic acid	-6.2
	Syringetin-3-rutinoside	-8.1		Tetracosanoic acid	-6.2
	Cycloartenol	-8.1		Nonanedioic acid	-6.2
	Caffeic acid 3-glucoside	-8.1		9-Tricosene	-6.1
	Quercetin-3-rutinoside	-8		Methyl-1,9-octadecenoate	-6.1
	Cycloeucaleanol	-7.8		Dodecanoic acid	-6.1
	Quercetin-3-rutinoside-7-rhamnoside	-7.7		Hexadecan-1-ol	-6.1
	α -Tocopherol	-7.5		Methyl hexadecanoate	-6
	Cycloeucalenone	-7.4		Hexadecanoic acid	-6
	2-methyl-5-(1-methylethyl)phenol	-7.2		Hexacosanoic acid	-6
	Trans-ferulic acid	-7.1		Octadecan-1-ol	-6
	Procyanidin B4	-7.0		Docosan-1-ol	-6
	L-dopa	-6.9		1-Nonadecene	-5.9
	2,6,10,14,18,22-Tetracohexaene	-6.9		3,5-dihydro-2-methyl-4H-pyran-4-one	-5.9
	Pentacosanoic acid	-6.9		Octacosan-1-ol	-5.9
	Caffeic acid	-6.9		Tetracosan-1-ol	-5.7
	Quinic acid	-6.8		Octanoic acid	-5.6
	1,2-Benzenedicarboxylic acid	-6.7		Senoside A	-5.2
	Tricosanoic acid	-6.7		5-(hydroxymethyl)-2-furaldehyde	-5.1
	Procyanidin B1	-6.6		Malic acid	-5.1
	Octadeca-9,12-dienoic acid	-6.6		2-hydroxy-gamma-butyrolactone	-4.8
	Triacotanoic acid	-6.6		Succinic acid	-4.7
	13-octadecenoic acid	-6.5		4H-pyran-4-one	-4.7
	Docosanoic acid	-6.5		Propionic acid	-3.9
	Octadeca-9,12,15-trienoic acid	-6.5		Acetic acid	-3.2
	Octadec-9-enoic acid	-6.5		Ethanimidic acid	-3.2
	Benzenepropanoic acid	-6.5			

Table II. 2D chemical structures and SMILES of the best binding compounds from PubChem.

Best binding compound	Chemical structure	SMILES
Sesamin		<chem>C1[C@H]2[C@H](CO[C@@H]2C3=CC4=C(C=C3)OCO4)[C@H](O1)C5=CC6=C(C=C5)OCO6</chem>
Asarinin		<chem>C1[C@H]2[C@H](CO[C@@H]2C3=CC4=C(C=C3)OCO4)[C@H](O1)C5=CC6=C(C=C5)OCO6</chem>
Quercetin-7-rutinoside		<chem>CC1[C@@H]([C@@H](C[C@@H](O1)OCC2[C@H]([C@@H](C[C@@H](O2)OC3=CC(=C4C(=C3)OC(=C(C4=O)O)C5=CC(=C(C=C5)O)O)O)O)O)O)O</chem>
Kaempferol-3-rutinoside		<chem>C[C@H]1[C@@H]([C@H]([C@H]([C@@H](O1)OC[C@@H]2[C@H]([C@@H]([C@H]([C@@H](O2)OC3=C(OC4=CC(=CC(=C4C3=O)O)O)C5=CC=C(C=C5)O)O)O)O)O)O</chem>
(-)-Epicatechin		<chem>C1[C@H]([C@H](OC2=CC(=CC(=C21)O)O)C3=CC(=C(C=C3)O)O)O</chem>
(+)-Catechin		<chem>C1[C@@H]([C@H](OC2=CC(=CC(=C21)O)O)C3=CC(=C(C=C3)O)O)O</chem>